An Experimental and Modeling Study of Humid Air Premixed Flames

Anuj Bhargava
e-mail: bhargaa@utrc.utc.com

Med Colket

William Sowa

United Technologies Research Center,
East Hartford, CT 06070

Kent Casleton

Dan Maloney

U.S. Department of Energy,
Federal Energy Technology Center,
Morgantown, WV 26507

An experimental and modeling study has been performed jointly by UTRC and DOE-FETC to determine the effect of humidity in the combustion air on emissions and stability limits of gas turbine premixed flames. This study focuses on developing gas turbine combustor design criteria for the Humid Air Turbine (HAT) cycle. The experiments were conducted at different moisture levels (0 percent, 5 percent, 10 percent, and 15 percent by mass in the air), at a total pressure of 200 psi, pilot levels (0 percent, 1 percent, 3 percent, and 5 percent total fuel), and equivalence ratio (0.4 to 0.8 depending on the moisture levels). The moisture levels were achieved by injecting steam into dry air well upstream of the fuel-air premixing nozzle. Computations were made for comparison to the experiments using GRI Mech 2.11 kinetics and thermodynamic database for modeling the flame chemistry. A Perfectly Stirred Reactor (PSR) network code was used to create a network of PSRs to simulate the flame. Excellent agreement between the measured and modeled NO_x (5–10 percent) was obtained. Trends of added moisture reducing NO_x and the effects of equivalence ratio and piloting level were well predicted. The CO predictions were higher by about 30–50 percent. The CO discrepancies are attributed to in-probe oxidation. The agreement between the data and model predictions over a wide range of conditions indicate the consistency and reliability of the measured data and usefulness of the modeling approach. An analysis of NO_x formation revealed that at constant equilibrium temperature, T_{eq}, the presence of steam leads to lower O-atom concentration which reduces "Zeldovich and N_2O" NO_x while higher OH-atom concentration reduces "Fenimore" NO_x. [S0742-4795(00)00703-1]

Introduction

The Advanced Turbine System (ATS) Program sponsored by the Department of Energy (DOE) has among its objectives the development of gas turbine-based power systems which reduce the cost of generating electricity while increasing gas turbine efficiency and lowering emissions.

One engine cycle under study is the advanced-cycle Humid Air Turbine (HAT) [1]. The definition and preliminary engineering of a HAT power cycle based on aeroderivative engine technology was undertaken by a United Technology Corporation team, Fluor Daniel, Inc., Texaco, and EPRI in 1991 [2]. This cycle, shown simplistically in Fig. 1, uses low temperature gas turbine exhaust heat as well as heat from within the cycle (intercooler and aftercooler) to supply heated water to a saturator. Here, the compressor discharge is humidified and then the water-vapor laden air passes through a recuperator and combustor and then to the turbine. Both the increased mass flow of the humid air and higher specific enthalpy of the mixture provide additional power but require no additional compression work from the turbine, resulting in efficiency and power output gains.

Several preliminary design studies have been performed on the HAT cycle [3]. HAT cycles were identified that had over 60 percent efficiency and emissions estimates that met the DOE goals. These emissions, however, were based on estimates of NO_x formation in the presence of water vapor. A series of experimental and modeling studies, described in the following sections, have been performed to characterize the effect of humidity on the emissions and combustion stability of HAT cycle configurations.

Contributed by the International Gas Turbine Institute (IGTI) of THE AMERICAN SOCIETY OF MECHANICAL ENGINEERS for publication in the ASME JOURNAL OF ENGINEERING FOR GAS TURBINES AND POWER. Paper presented at the International Gas Turbine and Aeroengine Congress and Exhibition, Indianapolis, IN, June 7–10, 1999; ASME Paper 99-GT-8. Manuscript received by IGTI March 9, 1999; final revision received by the ASME Headquarters May 15, 2000. Associate Technical Editor: D. Wisler.

Several studies have been undertaken to understand the influence of moisture in air on NO_x and CO emissions. Dryer [4], Miyauchi et al. [5], Touchton [6], Blevins and Roby [7], and Meyer and Grienche [8] have all investigated the influence of moisture on emissions under different operating conditions. Most of these studies have dealt with diffusion flames. In diffusion flames, it was concluded that almost all of the NO_x reduction took

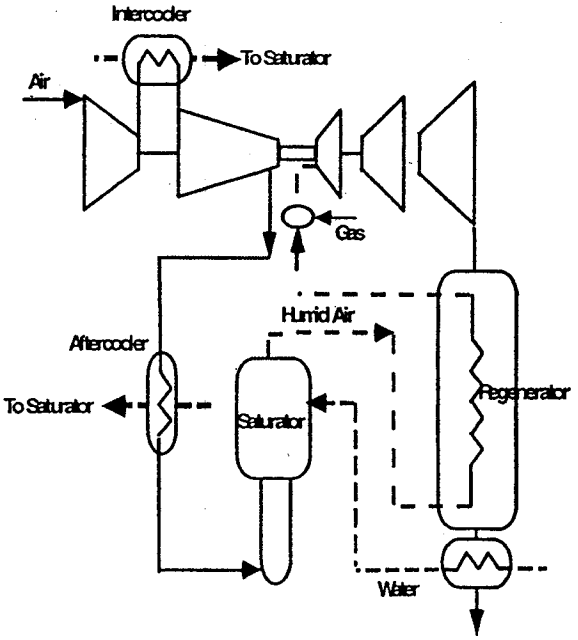

Fig. 1 A schematic of the HAT cycle

place due to a reduction in the flame temperature. In a diffusion flame, where the overall equivalence ratio may be as low as 0.4–0.5 the high temperature stoichiometric regions are the primary source of NO_x. Moisture reduces the peak temperatures which brings about a drastic reduction in NO_x emissions. Not much work has been carried out for premixed systems, required to meet low emissions regulation. Moisture addition into the air reduces NO_x emissions even in premixed systems. Initial investigation of premixed systems revealed several different pathways, which may account for the drastic reduction in NO_x emissions when moisture is increased. Some of the possible routes include:

- Reduction in equilibrium temperature (T_{eq}).
- Reduction of peak temperature of pilot diffusion flames.
- Equivalence ratio change. (In humid air flames for constant T_{eq}, as the moisture level increases, the equivalence ratio must increase resulting in a lower O-atom concentration.)
- Dilution effect. (In humid air flames for constant T_{eq}, as the moisture level increases, the O-atom and N_2 mole fraction ratios decrease.)
- O-atom suppression. (Presence of moisture promotes the reaction $O+H_2O \rightarrow OH+OH$, leading to O-atom suppression reducing NO_x through the "Zeldovich and N_2O pathways.")
- Heat release rate reduction lowering peak temperatures and super-equilibrium O-atom.

Experiments

Experiments were conducted in the Low Emissions Combustor Test and Research (LECTR) facility at the U.S. Department of Energy's Federal Energy Technology Center. The LECTR facility, Fig. 2, is a refractory lined pressure vessel containing test modules configured to meet specific test requirements. The facility was designed for pressurized operations up to 450 psig with access to a preheated (1000°F max) air supply capable of delivering up to 3.2 pps of air.

In the present test configuration, superheated steam was added to the preheated combustion air and then injected into an inlet plenum. The flow was straightened through a series of perforated metal plates and passed through the test nozzle where it was mixed with the primary fuel supply. Two diffusion flame pilot fuel streams were also employed. A side-wall pilot fuel flow was injected through the wall of the combustor approximately one half inch above the tip of the nozzle. In addition, center-body pilot fuel was injected along the centerline of the nozzle. Combustion products passed upward across an area-averaged sample probe which spanned the combustor diameter. The flow continued upward into a plenum where it turned 90 deg before entering a water quench zone where the gas temperature was reduced prior to passing through a pressure control valve and out an exhaust stack.

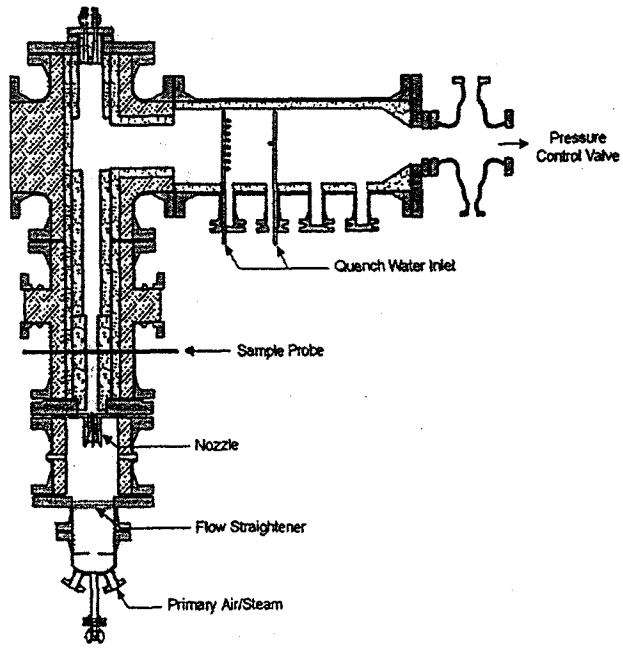

Fig. 2 A schematic of the experimental setup

Experiments were conducted to evaluate the emissions performance as a function of firing conditions for a two square inch effective flow area scaled version of the tangential entry fuel nozzle. Larger scale versions of the nozzle have been reported in the literature [9]. The two square inch effective area nozzle tests were conducted at 200 psi at an air flow of 2.2 pps and a combustor insert diameter of 4.25 in.

Test parameters examined included percentage of total fuel flow as side-wall pilot (0, 1, or 5 percent), percentage of total fuel flow as center-body pilot (0, 1, 3, or 5 percent), percentage of steam relative to combustion air (0, 5, 10, 15, or 20 percent) and air/steam mixture temperature (varied from 935 to 725°F depending on steam loading and air preheat). All percentages were taken as mass percent. All fuel, air and steam flows were measured using precision orifice runs with flow control valves tied to an automated control system. Excellent mass balance closure (typically within 1 to 2 percent) was observed when comparing input flow measurements with measured combustion product compositions.

Experiments were performed by establishing the required air and steam flows for a given test condition. The side-wall, center-body and main fuel flows were then set based on a prescribed equivalence ratio. The nozzle was held at the above condition for a period of 10 to 15 min to establish a steady baseline. The three fuel streams were then simultaneously ramped to lower flows (leaner conditions) keeping their relative ratios constant while the air and steam flows remained fixed. Fuel ramp rates were established based on the gas sample system response time and typically involved reducing fuel flow approximately 30 percent during a one-hour ramp. The starting equivalence ratios for these tests were selected based on previous experience with the test nozzle to give a starting CO emission level of 50 ppm or greater. As the fuel was ramped to leaner conditions, CO emissions passed through a minimum and rose rapidly as the lean blow-off limit was approached. Fuel ramps were discontinued when CO levels exceeded 200 ppm. As steam loading in the combustion air was increased the starting equivalence ratio was increased as well to stay on the rich side of the CO minimum.

Gas samples were obtained using water cooled rake probes designed to extract representative gas samples across the area of the combustor. The sample probe was located approximately 15 in above the nozzle tip. Extracted gas samples were transported through heated transfer lines to a pressure let-down station followed by a chiller to remove water. The dried sample gas was then passed through an analyzer train configured to measure O_2, CO_2, CO, total NO_x, and Unburned Hydrocarbons.

Modeling

Experimental data covered a wide range of equivalence ratios and humidity levels. The fuel concentration in the pilots was also varied from 0 percent to 5 percent fuel in the pilot to determine the optimum level of side pilot required to keep NO_x emissions low, but provide enough stability to the lean flame. Some of the observations made from the experiments were as follows:

For dry flames at constant T_{eq}:

- NO_x emissions increase with increasing fuel in the pilot while CO emissions show no dependence on pilot level

For humid air experiments:

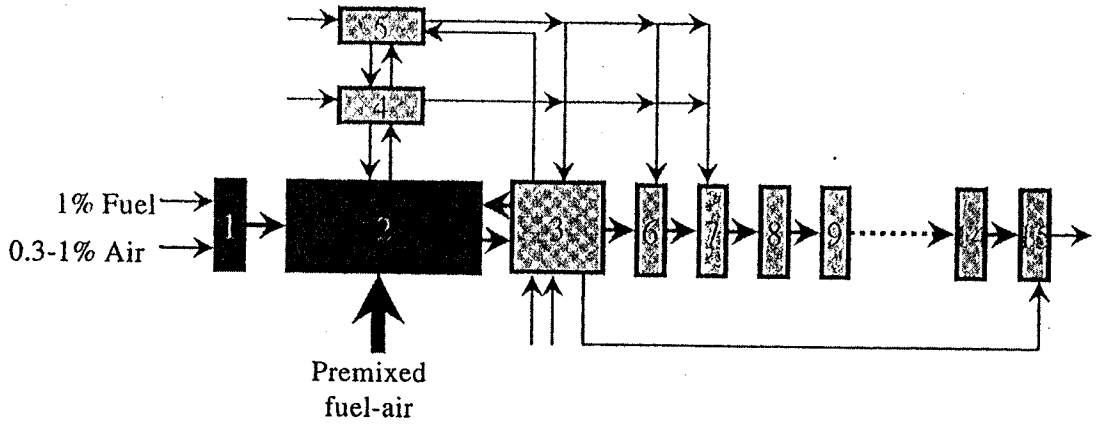

Fig. 3 A schematic of the PSR reactor network used to model the flame

- NO_x and CO levels decrease with increase in the humidity levels
- similar effect of pilot levels as in dry flames

The experiments were modeled using a literature reaction set, GRI Mech2.11 (Bowman et al. [10]) and its accompanying thermochemistry. GRI Mech2.11 reaction set consists of 49 species and 277 reactions and has been validated over a wide range of pressure and equivalence ratios. A PSR Network code developed at UTRC was used to simulate the combustor. The basis for the Network PSR code is the Chemkin PSR model [11]. The Network used to model the experiment is shown in Fig. 3. The network was designed to simulate the mixing and flow characteristics of the experiment, as closely as possible. A total of 15 reactors were used to represent the combustor. The number 15 was arbitrarily chosen to simulate the process in a reasonable manner without a high computational burden. The combined volume of the 15 reactors gave a residence time equal to the experimental residence time in the equipment. A small amount of fuel and air mixture was introduced in the first reactor. This represented the central pilot. The products of reactor 1 along with most of the fuel (75 to 79 percent) and air (80 to 90 percent) were introduced in reactor 2. Twenty percent of the fuel along with 10 percent of air enters the system through reactor 3. The combination of reactors 2 and 3 represent the inhomogeneity that may be present due to less than perfect mixing. Reactors 2 and 3 represent the flame zone. The side pilot was simulated by flowing 0–5 percent of the fuel through reactors 4 and 5. Providing recycle between reactors 2 and 4 simulated recirculation. The rest of the reactors (6 to 15) represent the post-flame zone. NO_x is primarily formed in reactors 2 and 3 while the rest of the reactors, 4 to 15, are for mixing of the side and central pilots with the flame and for CO burnout. In this manner the network was designed to match experimental NO_x and CO. Residence time varied with flow rates as air was fixed while the fuel flow rate was changed in order to achieve the required equivalence ratio. Residence time in each reactor was a function of the flow rate through the reactor and reactor volume. The residence time in all the reactors combined was between 4.5 and 6 ms. The flame zone (reactor 2 and 3) accounted for most of the residence time (nearly 60 percent). The network structure remained the same for all conditions but minor alterations for fuel/air distribution had to be done from one case to another to stabilize the network and to simulate the flow characteristics. For example, with very fuel lean conditions or for cases with 10–15 percent moisture, fuel in the first reactor had to be increased to stabilize the network. With different fuel flows across the pilot, fuel and/or air distribution in reactor 2 and 3 had to be slightly modified.

Solutions were compared with experiments on the basis of combustor exit temperature which is equal to T_{eq} based on local equivalence ratio. The combustor exit temperature in general is different from the local temperature in the PSR as the local temperature can be kinetically limited.

Results and Discussion

Numerous experiments were performed to ascertain the effect of moisture, equivalence ratio, and inlet temperature on the amount of NO_x and CO formed. The effect of pilot level (0, 1, 3, 5 percent fuel) and moisture level (0, 5, 10, 15 percent water in the air by mass) on NO_x and CO emissions can be seen in Figs. 4 to 7.

As seen in Fig. 4, higher side pilot levels lead to higher NO_x. The effect is more pronounced at very lean conditions. This result agrees well with the findings of Leonard and Stegmaier [12], and Maghon et al. [13]. Further analysis of the NO_x formed at different pilot levels in this study indicated that with one percent increase in the fuel injected through the side pilot, NO_x emissions go up by 1.5 ± 0.2 ppm. This increase is less than the increase observed by Maghon et al. [13]. CO emissions remain more or less unaffected by the pilot level, as observed in Fig. 5. The effect of moisture level in the air is seen in Figs. 6 and 7. NO_x and CO emissions show a significant drop with increasing amounts of moisture in the air stream. Much of the reduction shown in these figures can be attributed to a reduction in flame temperatures at constant ϕ, with increasing moisture. As will be shown later, even at constant flame temperature, NO_x and CO is reduced with increasing moisture levels.

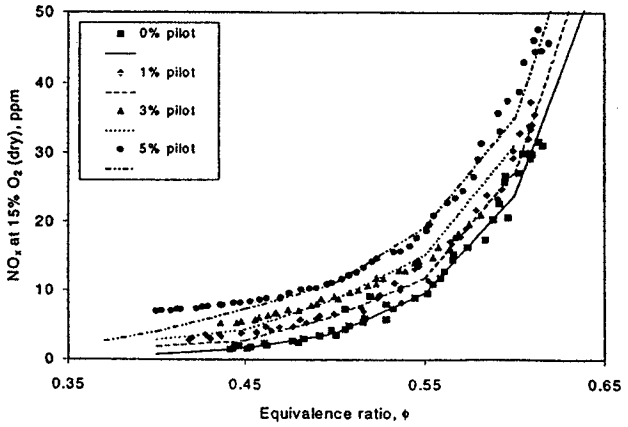

Fig. 4 Comparison between measured NO_x and computed NO_x at 200 psi at different pilot levels

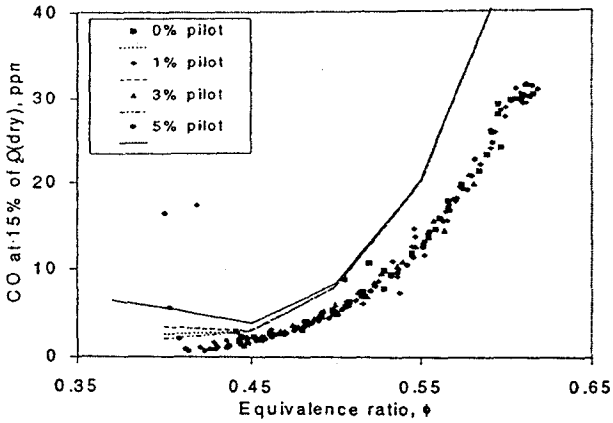

Fig. 5 Comparison between measured CO and computed CO at 200 psi at different pilot levels

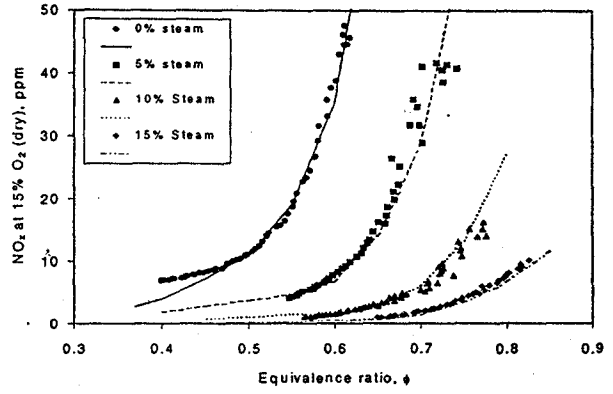

Fig. 6 Comparison between measured and computed NO_x for a 5 percent side pilot flame at 200 psi for different steam loading

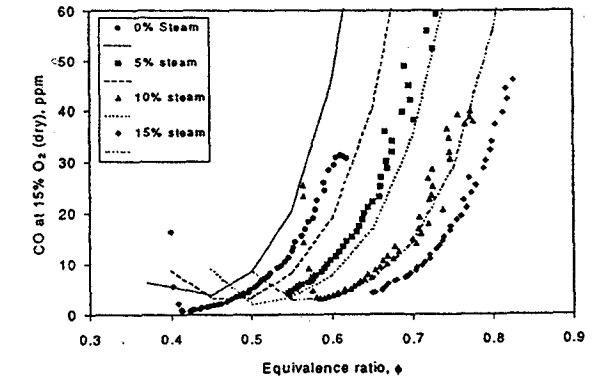

Fig. 7 Comparison between measured and computed CO for a 5 percent side pilot flame at 200 psi for different steam loading

Simulations examined the influence of pilot and humidity level consistent with the experiments. Figs. 4 and 5 show the comparison between the experiments and modeling as piloting level varies. NO_x predictions are very good but the predictions for CO are off by as much as 50 percent. This trend was observed in all simulations. The CO predictions were close to the equilibrium levels and are highly sensitive to the mixture (air and fuel) temperature. A small (~50°F) discrepancy in the measured air-fuel temperature can account for the difference in the measured and computed CO. Alternatively, the sample probe's impact on the equilibrating CO which is still undergoing reaction may explain the lower experimental values. Small levels of additional CO destruction in the probe could also explain the discrepancy. A study of the probe effect on CO measurements has been presented by Nguyen et al. [14]. Nguyen et al. measured CO in an atmospheric pressure flame using line-of-sight tunable diode laser absorption and extractive probe sampling and compared it with CO prediction using a numerical model. They found that the measurements made with extractive sampling technique were as much as 10 times less than the laser-based experiments for fuel-lean flames whereas for fuel-rich flames the agreement between the two techniques was good.

The same network design developed for the dry air cases was extended to humid air cases. Shown in Figs. 6 and 7 are the comparison for NO_x and CO mole fraction measured in the flame and simulated by the network. Higher humidity brings about a drastic reduction in the formation of NO_x. As the amount of moisture increases, the lean blowout limit moves to higher equivalence ratios consistent with the shift seen in Figs. 6 and 7. For a dry air flame at $T_{air}=860°F$ and at $P=200$ psi, the boundary between equilibrium CO and the onset of lean blow out dynamics occurs at an equivalence ratio of 0.41. This boundary shifts as more moisture is introduced. It goes up to 0.55 for 5 percent moisture and to 0.65 for 15 percent moisture in the air stream. The network PSR is able to capture the behavior of the NO_x concentrations to within 5–10 percent of the measurements, further corroborating the modeling approach. CO predictions are higher (20–40 percent) than the measurements. This effect was similar to the one seen in the piloting data.

As seen in Fig. 7, flame stability limits move to higher equivalence ratios as moisture content increases. Moisture in the air reduces flame temperatures. Flames with different humidity levels have different temperatures for the same equivalence ratio. For example, a 0.54 equivalence ratio flame with no steam has the same T_{eq} as a flame with 15 percent steam in the air at an equivalence ratio of 0.75. Another method, therefore, of comparing flames is to compare NO_x and CO emissions formed in flames at different moisture levels as a function of T_{eq}. The computations of T_{eq} were carried out using equilibrium code called STANJAN, developed by Reynolds [15] and modified by Kee and Lutz [16]. The computation included 49 species. The GRI 2.11 thermodynamic database was used for these computations. The temperatures in Figs. 8 and 9 (and also Figs. 10 and 11) are the T_{eq} for the entire fuel-air mixture in the combustor. Actual flame temperatures in the experiment are distributed and somewhat lower due to heat losses to the burner and surrounding air in the chamber. Figures 8 and 9 indicate the dependence of NO_x and CO on T_{eq}. As seen in Fig. 8, calculations and measurements indicate that a

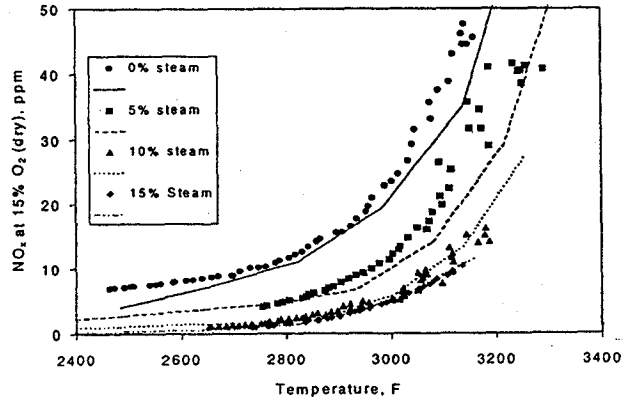

Fig. 8 Comparison between measured and computed NO_x for a 5 percent side pilot flame at 200 psi for different steam loading

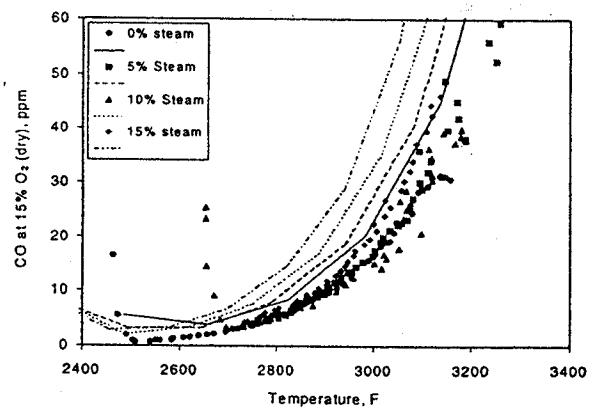

Fig. 9 Comparison between measured and computed CO for a 5 percent side pilot flame at 200 psi for different steam loading

dry air flame at $\phi = 0.54$ would have a T_{eq} of 2950°F and NO_x emissions of around 15 ppm. At the same time, a flame with humid air (15 percent steam content) at $\phi = 0.75$ has the same T_{eq} of 2950°F, but its NO_x emissions are only 3 ppm. This means that besides reducing NO formation in flames by reducing the flame temperature [6,7], humidity also reduces NO by some other mechanism. This reduction can be due to the change in the radical pool because of varying amounts of moisture and different equivalence ratios at the same temperature, or due to any of the other factors mentioned in the introduction. The flame at 0.54 equivalence ratio (dry air) is richer in O-atom than a humid air flame (15 percent steam) at 0.75 equivalence ratio, even though both flames are at the same T_{eq}. One of the other possibilities which can account for the drastic reduction in NO_x is the temperature attained in each of the PSR's in the network. As mentioned in the introduction, moisture in the feed stream can slow heat transfer rates, and, hence, a different moisture content can lead to a different maximum temperature (residence time in the different

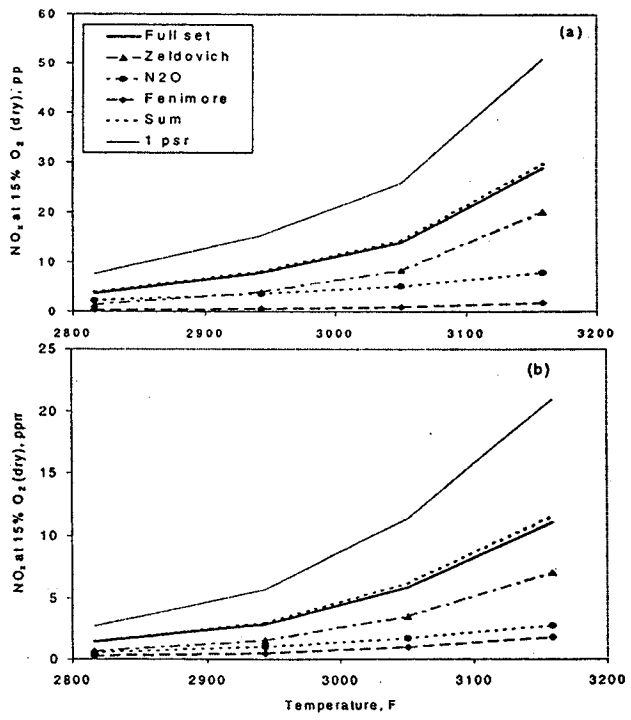

Fig. 10 Influence of different pathways on NO_x formation for a flame with a 0 percent side pilot and (*a*) 0 percent steam and (*b*) 15 percent steam. Calculations with one psr also shown for comparison purposes.

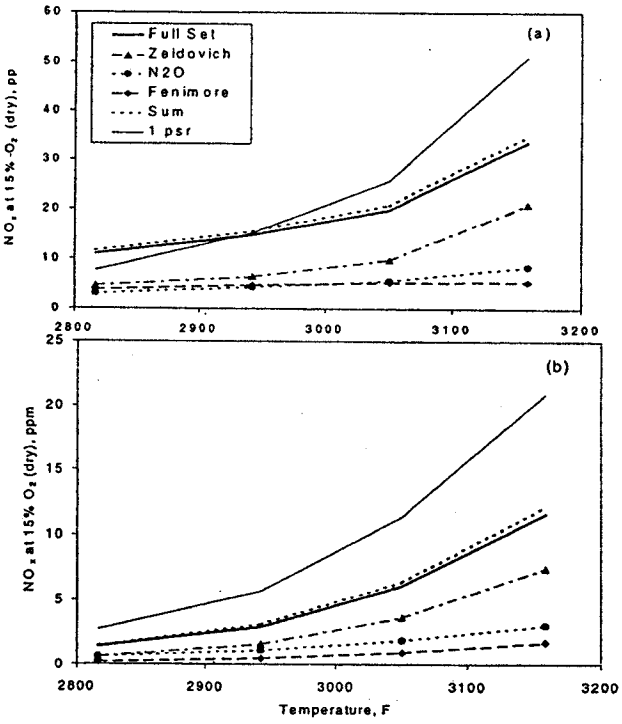

Fig. 11 Influence of different pathways on NO_x formation for a flame stabilized by a 5 percent side pilot and (*a*) 0 percent and (*b*) 15 percent steam. Calculations with one psr also shown for comparison purposes.

PSR's is fixed) attained in PSR 2 and PSR 3 of the network, which account for most of the NO_x formed. An analysis of the temperatures attained in the different PSR's in the network, for flames with different moisture content but at the same T_{eq}, indicated that moisture content does not alter the temperature attained in each of the reactors. Hence, a reduction in NO_x concentration with increased moisture content is not due to lowering of peak temperatures in the reactors. CO emission levels at one T_{eq} do not vary with humidity, as seen in Fig. 9.

To determine the roles of various mechanisms on the production of NO_x, several modifications were made to the reaction set. NO_x formation reactions were divided into three different but coupled groups as follows:

1 "Zeldovich or thermal NO_x Mechanism" [17] as extended by Bowman and Seery [18]. NO_x in Zeldovich or thermal NO_x mechanism is initiated by the reaction of N_2 with O. This well known three-step reaction sequence is the dominant NO_x forming route at temperatures above 2950°F. Zeldovich or thermal NO_x mechanism was suppressed by making the reaction $N+NO \rightarrow N_2+O$ proceed in the forward direction only.

2 "N_2O Mechanism" consisting of reactions involving N_2O which form NO. NO_x formed via this mechanism can be effectively suppressed by making the $N_2O(+M) \rightarrow N_2+O(+M)$ proceed in the forward direction only.

3 The third mechanism responsible for NO_x formation is "Fenimore NO" [19]. All NO_x forming reactions, beside the "Zeldovich and N_2O" pathways, are included in this route. The main steps influencing this reaction sequence are $N_2+CH=HCN+N$, $N_2+CH_2=HCN+NH$, and other reactions involving N_2 and hydrocarbon radicals. This extensive sequence was suppressed by inhibiting the forward rates for reactions between hydrocarbon fragments and molecular nitrogen.

The NO_x formation rates of each of these reaction sequences can be enhanced through super-equilibrium levels of O-atoms and other radical species in the flame front.

To study the contribution of each pathway, the other two channels were suppressed. Hence, in order to analyze the importance of "Zeldovich Mechanism," NO_x formation via "Fenimore and N_2O Mechanisms" was removed. Similar computations were performed to evaluate the importance of "Fenimore and N_2O Mechanisms." The analysis was carried out for 0 percent and 5 percent pilot levels at 0 percent and 15 percent moisture loading. Figures 10 and 11 show the contributions of the different mechanisms for the four cases. Also shown in the figures is the NO_x computed with a single PSR. The differences between these calculations and those of the network analysis indicates the effect of mixing in the combustion chamber and circulation on NO_x formation and finite reaction times required to approach T_{eq}. The NO_x prediction for the 1 PSR case is higher than the Network PSR, primarily due to residence time distribution. In the Network, reactors 2 and 3 are the reactors primarily responsible for making NO_x and CO. In order to simulate the experiments with the network, reactor volume (which determines the residence time in the reactor) was used as one of the adjustable parameters. Once established for one case, the volumes were not changed for any of the other cases. Hence, by keeping the residence time low, one may inhibit NO_x generation. On the other hand, in the case of 1 PSR, the residence time was not a variable and was the same as the whole of the network combined.

"Zeldovich NO_x" dominated the other NO_x formation channels in the temperature range studied, except for the 0 percent side pilot flame for dry air. For this case, seen in Fig. 10(*a*), "N_2O Pathway" dominates the "Zeldovich Pathway" in the lean operating range (2800 to 2900°F). This is the range in which most of the industrial gas-turbines operate.

Figure 10 shows the behavior of NO_x formed at two moisture levels, 0 and 15 percent, for flames with 0 percent fuel coming in from the side pilot. As seen in the figure, at temperatures around 2950°F, NO_x formed by the N_2O pathway is comparable to the "Zeldovich or thermal" NO_x, but at temperatures around 3050°F, "Zeldovich" NO_x starts increasing much more rapidly and becomes the dominant NO_x formation channel. Comparing the NO_x formed in the flames with and without moisture, it can be seen that at the same temperature, NO_x formed in the cases with 15 percent moisture is much less than the NO_x formed in dry air flames. At temperatures around 2800°F the decrease is close to a factor of 8 while at higher temperatures it is around a factor of 3. These calculations indicate that NO_x formed decreases in flames with added moisture as compared to dry flames even when the T_{eq} for the two flames is the same. This suggests that all the reduction in NO_x cannot be attributed to thermal effects (as defined by T_{eq}).

The decrease in the "Zeldovich and N_2O" NO_x can be attributed to the reduction in O atom concentration. As mentioned earlier in the paper, at the same equivalence ratio the high humidity flames are of lower temperatures than dry flames. Hence, in order to evaluate the different flames at the same temperature, high humidity flames had to be at a higher equivalence ratio than dry flames. Scarcity of O_2, and, hence, lower O atom in the higher equivalence ratio humid flames would lead to lower NO_x formation by the "Zeldovich and N_2O Mechanism." Humidity promotes $O+H_2O$ reaction, and, hence, suppresses O-atom concentration. A reduction in the "Fenimore" NO_x can be attributed to the change in the OH radical concentration in the flame. Higher OH concentration in humid air flames promotes oxidation of the hydrocarbon radicals [5], which would reduce "Fenimore" NO. Similar behavior was seen in the 5 percent side pilot flame too (Fig. 11). Due to the side pilot, NO_x levels were higher than the flame with no side pilot. The increase in NO_x for the flame with 5 percent fuel coming in from the side pilot was more predominant at the lower temperatures and was mostly due to higher Fenimore NO at the lean conditions (especially for the dry flame).

The factors mentioned in the introduction were also considered. There is definitely some reduction in NO_x due to lowering of temperature. Reduction of the peak temperature of the side pilot can also reduce NO_x formation, though the analysis with 0 percent side pilot indicates that this may not be the dominant factor. Suppression and delay of heat transfer rates due to added moisture would slow down the combustion process and lower super-equilibrium O-atom concentration and temperatures in reactors 2 and 3. These two reactors account for most NO_x formation and a lower temperature in these reactors (even though T_{eq} for the whole flame could be the same as the case with dry air) would lead to lower overall NO_x. Lower super-equilibrium O-atom concentrations would also lead to lower NO_x (reduction in "Zeldovich and N_2O" NO_x).

The percentage of NO reduction from the three mechanisms was similar for dry run and for humid air run. This indicates that even with moisture addition, which has the effect of lowering T_{eq}, the thermal NO channel remained the most dominant NO formation channel for most of the conditions examined in this study.

Conclusions

Data were collected over a wide range of equivalence ratio, moisture in the air stream, and pilot levels. The trends in the measured data have been used to evaluate the effect of various parameters on NO_x and CO emissions. The data have also been modeled using a PSR network and a literature reaction set. Good match between the data and modeling suggests that the approach used for modeling the combustor is useful. Addition of moisture to the air stream brings about a significant reduction in NO_x emissions. This reduction in NO_x is primarily due to a decrease in the T_{eq}, but reduction in NO_x with increasing moisture is also observed for flames in which T_{eq} is held constant. Analysis of the reaction set and computations for the three different NO_x formation pathways indicate the importance of O-atom concentration on NO_x formation. Moisture loading of 15 percent in the air reduces NO_x emissions by as much as a factor of 3 to 8 (depending on the T_{eq}) at the same T_{eq} as a dry flame. This reduction is attributed to the decrease in O-atom concentration. Even with 15 percent moisture content, most of the NO_x formation takes place via the "Zeldovich" pathway.

Acknowledgements

This work was supported by DOE/METC under contract DE-AC21-96MC33084. The authors would also like to thank Fred Robson, Brian Knight, and Archer Jennings for helpful discussions.

References

[1] Rao, A. D., 1989, "Process for Producing Power," US Patent 4,829,763, May 1989.

[2] Humid Air Turbine (HAT) Cycle Public Report, Turbo Power and Marine (TPM), April, 1993.

[3] Robson, F. L., 1993, "Advanced Turbine Systems Study-System Scoping And Feasibility Study," DOE Contract DE-AC21-92MC29247, United Technologies Research Center, East Hartford, CT.

[4] Dryer, F. L., 1976, "Water Addition to Practical Combustion Systems-Concepts and Applications," *Sixteenth Symposium (International) on Combustion*, The Combustion Institute, Philadelphia, PA.

[5] Miyauchi, Y., Mori, Y., and Yamaguchi, T., 1981, "Effect of Steam Addition on NO Formation," *Eighteenth Symposium (International) on Combustion*, The Combustion Institute, Pittsburgh, PA.

[6] Touchton, G. L., 1985, "Influence of Gas Turbine Combustor Design and Operating Parameters on Effectiveness of NO_x Suppression by Injected Steam or Water," ASME Paper 84-JPGC-GT-3.

[7] Blevins, L. G., and Roby, R. J., 1995, "An Experimental Study of NO_x Reduction in Laminar Diffusion Flames by Addition of High Levels of Steam," ASME Paper 95-GT-327.

[8] Meyer, J.-L., and Grienche, G., 1997, "An Experimental Study of Steam Injection in an Aeroderivative Gas Turbine," ASME Paper 97-GT-506.

[9] Kendrick, D. W., Anderson, T. J., Sowa, W. A., and Snyder, T. S., 1998, "Acoustic Sensitivities of Lean-Premixed Fuel Injectors in A Single Nozzle Rig," ASME Paper 98-GT-382.

[10] Bowman, C. T., Hanson, R. K., Davidson, D. F., Gardiner, W. C., Jr., Lissianski, V., Smith, G. P., Golden, D. M., Frenklach, M., and Goldenberg, M., 1994, http://www.me.berkeley.edu/gri_mech/

[11] Glarborg, P., Kee, R. J., Grcar, J. F., and Miller, J. A., 1988, "PSR: A Fortran

Compiler for Modeling Well-Stirred Reactors," Sandia National Laboratories Report, SAND86-8209, Livermore, CA.
[12] Leonard, G., and Stegmaier, J., 1994, "Development of an Aeroderivative Gas Turbine Dry Low Emissions Combustion Systems," ASME Paper 93-GT-288.
[13] Maghon, H., Berenbrink, P., Termuehlen, H., and Gartner, G., 1990, "Progress in NO_x and CO Emission Reduction of Gas Turbines," ASME Paper 90-IPGC/GT-4.
[14] Nguyen, Q. V., Edgar, B. L., Dibble, R. W., and Gulati, A., 1995, "Experimental and Numerical Comparison of Extractive and In Situ Laser Measurements of Non-Equilibrium Carbon Monoxide in Lean-Premixed Gas Combustion," Combust. Flame, **100**, pp. 395–406.
[15] Reynolds, W. C., 1981, "STANJAN,"Interactive Computer Programs for Chemical Equilibrium Analysis, Stanford University, Stanford, CA.
[16] Kee, R. J., and Lutz, A., private communication.
[17] Zeldovich, J., 1946, "The Oxidation of Nitrogen Combustion and Explosions," Acta Physicochim. URSS, **21**, p. 577.
[18] Bowman, C. T., and Seery, D. J., 1972, *Emissions from Continuous Combustion Systems*, W. Cornelius and W. G. Agnew, eds., Plenum, New York, p. 123.
[19] Fenimore, C. P., 1971, "Formation of Nitric Oxide in Premixed Hydrocarbon Flames," *Thirteenth Symposium (International) on Combustion*, The Combustion Institute, Philadelphia, PA.